ELSEVIER

Journal of Neuroscience Methods 156 (2006) 322–332

JOURNAL OF NEUROSCIENCE METHODS

www.elsevier.com/locate/jneumeth

Detecting time-dependent coherence between non-stationary electrophysiological signals—A combined statistical and time–frequency approach

Yang Zhan [a,1], David Halliday [a], Ping Jiang [e], Xuguang Liu [b], Jianfeng Feng [c,d,*]

[a] *Department of Electronics, University of York, York YO10 5DD, UK*
[b] *Charing Cross Hospital & Division of Neuroscience and Mental Health, Imperial College London, London W6 8RF, UK*
[c] *Department of Mathematics, Hunan Normal University, 410081 Changsha, PR China*
[d] *Department of Computer Science and Mathematics, Warwick University, Coventry CV4 7AL, UK*
[e] *Department of Information and Control Engineering, Tongji University, 1239 Siping Road, Shanghai, 200092, China*

Received 6 December 2005; received in revised form 3 February 2006; accepted 13 February 2006

Abstract

Various time–frequency methods have been used to study time-varying properties of non-stationary neurophysiological signals. In the present study, a time–frequency coherence estimate using continuous wavelet transform (CWT) together with its confidence intervals are proposed to evaluate the correlation between two non-stationary processes. The approach is based on averaging over repeat trials. A systematic comparison between approaches using CWT and short-time Fourier transform (STFT) is carried out. Simulated data are generated to test the performance of these methods when estimating time–frequency based coherence. In contrast to some recent studies, we find that CWT based coherence estimates do not supersede STFT based estimates. We suggest that a combination of STFT and CWT would be most suitable for analysing non-stationary neural data. Tests are presented to investigate the time and frequency discrimination capabilities of the two approaches. The methods are applied to two experimental data sets: electroencephalogram (EEG) and surface electromyogram (EMG) during wrist movements in a healthy subject, and local field potential (LFP) and surface EMG recordings during resting tremor in a Parkinsonian patient. Supporting software is available at http://www.dcs.warwick.ac.ukffeng/software/COD and http://www.neurospec.org.

Keywords: Wavelet; Fourier; Coherence; Confidence intervals; EEGs; EMGs; LFPs; Time discrimination; Frequency discrimination

1. Introduction

Coherence analysis has been extensively applied to the study of neural activity. Neurophysiological signals contain noise at all levels and are treated as random signals or stochastic processes (Lin and Chen, 1996). A single stationary stochastic process is often characterised by its autocovariance function and its power spectrum. The power spectrum is the Fourier transform of the autocovariance function and provides a frequency description of the process. The frequency or spectral contents of neural signals display important information and have been used to evaluate physiological and functional states of the nervous system. Fourier analysis has been used extensively in studying the spectra of neurophysiological signals and in recent years interest has been focused on the study of correlated phenomena between two or more signals, such as synchronisation between brain areas (Andrew and Pfurtscheller, 1996; Shibata et al., 1998) and correlation between electroencephalogram (EEG), electromyogram (EMG) and magnetoencephalogram (MEG) (Halliday et al., 1998; Mima and Hallett, 1999; Mima et al., 2000; Grosse et al., 2002). In general, the investigated signals or data are assumed to be stationary and the estimates of the auto and cross spectra are calculated to obtain the coherence estimate. Based on Fourier analysis and under Gaussian assumption, confidence intervals of the estimated coherence can be estimated. The construction of the confidence intervals is of vital importance since it allows significant correlation to be detected and statistically assessed at various frequency ranges.

* Corresponding author. Tel.: +44 7799572480.
E-mail address: jianfeng.feng@warwick.ac.uk (J. Feng).
[1] Present address: Laboratory of Cognitive and Behavioural Neuroscience, The Babraham Institute, Cambridge CB2 4AT, UK.

0165-0270/$ – see front matter © 2006 Elsevier B.V. All rights reserved.
doi:10.1016/j.jneumeth.2006.02.013

A wide range of neural signals encountered in biomedical applications fall into the category of non-stationary signals whose statistical properties change with time. Traditional Fourier analysis provides no information about evolution of frequency components over time. Short-time Fourier transform (STFT), a method which applies a short-time window to the signal and performs a series of Fourier transforms within this window as it slides across all the data, can overcome this limitation, providing a time–frequency representation of the signal. Alternatively, wavelet transforms provide a useful approach in investigating non-stationary signals, this is often regarded as an "optimal" solution with regard to time and frequency resolution. Wavelet analysis has previously been used to study EEG (Samar, 1999; Lambertz et al., 2000; Senhadji and Wendling, 2002; Slobounov et al., 2000) and EMG (Pope et al., 2000; Karlsson et al., 2003). Transform methods based on Fourier and wavelet analysis are compared in Bruns (2004) in the context of neural data. Correlation detection based on wavelet transforms has been used in wind engineering (Gurley et al., 2003) and climatic and oceanic research (Torrence and Webster, 1999). In recent years in connection with neurophysiological applications, wavelet based cross spectral and coherence analysis have been used to analyse spike train activity (Pezaris et al., 2000; Lee, 2002).

The main contribution of this paper is the following. First, a time–frequency coherence based on continuous wavelet transform (CWT) using averaging over repeat trials is proposed, and a way of estimating confidence intervals is described. Second, simulation studies are used to compare the relative merits of CWT and STFT approaches. Similar results are obtained with both approaches. However, our results indicate that STFT gives higher coherence values at low frequencies (<10 Hz) compared to CWT based estimates. Third, statistical tests are introduced to determine the relative abilities of STFT and CWT based coherence estimates to resolve components in frequency and time. Results from applying these tests to simulated data indicate that CWT generally outperforms STFT. Previous results presented in the literature suggest CWT has a clear advantage over STFT. Although it has been shown that STFT and CWT approaches are mathematically equivalent (Bruns, 2004), for any particular parameter set the methods partition the time–frequency plane in a different manner, in particular the CWT uses a variable length data window at each frequency (or scale). Based upon our results, we suggest that a more reasonable approach to detect the time-varying coherence between two signals would be to consider both STFT and CWT approaches.

Our approach is then applied to two sets of experimental data: EEG-EMG obtained from healthy subjects during a voluntary wrist movement task (Halliday et al., 1998), and LFP-EMG obtained from Parkinson's disease patients during involuntary resting tremor (Liu et al., 2002, 2003). We expect that our approach could reveal some fundamental facts with large data sets, for example, LFPs recorded from a multi-electrode array (Horton et al., 2005; Feng, 2004; Tate et al., 2005).

2. Methods

2.1. Time–frequency coherence

2.1.1. Continuous wavelet transform and short-time Fourier trans-from

The continuous wavelet transform of $x(t)$ is defined as

$$\mathrm{CWT}_x(a,b) = \int_{-\infty}^{\infty} x(t)\psi^*_{a,b}(t)\,\mathrm{d}t \tag{1}$$

where

$$\psi_{a,b}(t) = \frac{1}{\sqrt{a}}\psi\left(\frac{t-b}{a}\right) \tag{2}$$

$\psi(t)$ is called the mother wavelet where a is the dilation parameter, b is the location parameter and * denotes complex conjugate. The choice of the wavelet should satisfy a number of selection criteria, such as the candidate functions having finite energy (the integral of the magnitude squared over time must be finite) and satisfying an admissibility condition (Addison, 2002).

The CWT is usually presented as a time–frequency representation by converting the scale parameter to frequency. To fulfil this representation, a characteristic frequency, f_0, defined as the bandpass centre or central frequency of the wavelet energy spectrum is chosen. The relationship between the frequency and scale is then $f = f_0/a$ (Addison, 2002). The CWT can be expressed as

$$\begin{aligned}\mathrm{CWT}_x(\tau, f) &= \mathrm{CWT}_x(a,b)|_{a=f_0/f, b=\tau} \\ &= \sqrt{\frac{f}{f_0}}\int_{-\infty}^{\infty} x(t)\psi^*\left(\frac{t-\tau}{f_0}\right)\,\mathrm{d}t\end{aligned} \tag{3}$$

One of the most commonly used wavelets in practice is the Morlet wavelet, defined as

$$\psi(t) = \frac{1}{\pi^{1/4}}(\mathrm{e}^{\mathrm{j}2\pi f_0 t} - \mathrm{e}^{-(2\pi f_0)^2/2})\mathrm{e}^{-t^2/2} \tag{4}$$

where f_0 is the central frequency of the wavelet. If the choice of f_0 is appropriate the second term in the bracket, which is known as the correction term becomes negligible, thus giving a simple Morlet wavelet (Kronland-Martinet et al., 1987)

$$\psi(t) = \frac{1}{\pi^{1/4}}\mathrm{e}^{\mathrm{j}2\pi f_0 t}\mathrm{e}^{-t^2/2} \tag{5}$$

This expression shows that Morlet wavelet is a complex sine wave within a Gaussian envelope. The Fourier transform of the Morlet wavelet is

$$\hat{\psi}(f) = \pi^{1/4}\sqrt{2}\mathrm{e}^{-(1/2)(2\pi f - 2\pi f_0)^2} \tag{6}$$

which has the form of a Gaussian function centred at f_0, where f_0 determines the wave numbers within the envelope. Here $f_0 = 0.849$, this gives a real part where the peaks next to the central peak are half the amplitude of the central peak. In Fig. 1a Morlet wavelet with $f_0 = 0.849$ and its Fourier transform are shown.

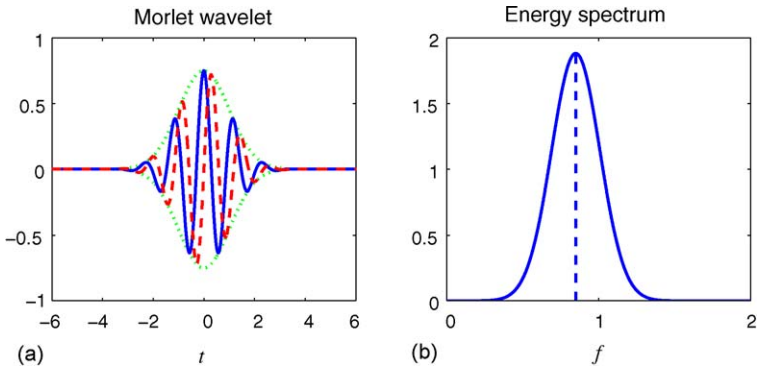

Fig. 1. Morlet wavelet and its Fourier transform, $f_0 = 0.849$. (a) Morlet wavelet. The solid line is the real part and the dashed line is the imaginary part. The dotted line is the envelope. (b) Fourier transform of Morlet wavelet, with the vertical dashed line corresponding to the characteristic frequency f_0.

By employing the convolution theorem the wavelet transform can be expressed as the product of the Fourier transforms of the signal and wavelet, $\hat{x}(f)$ and $\hat{\psi}(f)$

$$\mathrm{CWT}_x(a, b) = \sqrt{a} \int_{-\infty}^{\infty} \hat{x}(f)\hat{\psi}^*(af)\mathrm{e}^{\mathrm{j}2\pi fb}\,\mathrm{d}f \tag{7}$$

This relationship provides a convenient way to implement the CWT, since the Fourier transform of the wavelet function $\hat{\psi}_{a,b}(f)$ is known in analytic form. The computation only requires an FFT of the original signal and an inverse FFT of the product of $\hat{x}(f)$ and $\hat{\psi}^*(a, f)$.

The square modulus of the wavelet transform is often called the scalogram and is defined as

$$\mathrm{SCAL}_x(\tau, f) = |\mathrm{CWT}_x(\tau, f)|^2 \tag{8}$$

The scalogram is a time-varying spectral representation, which describes the energy distribution of the signal. The scalogram $|\mathrm{CWT}_x(\tau, f)|^2$ is often used to give an estimate of the wavelet spectrum (Torrence and Compo, 1998; Addison, 2002). The wavelet spectrum gives a time–frequency representation, and it measures the contribution to the total energy coming from the vicinity of a point at a specific time and frequency for a given mother wavelet (Perrier et al., 1995).

Another commonly used time–frequency representation is the short-time Fourier transform (Qian, 2002), defined as

$$\begin{aligned}\mathrm{STFT}_x(\tau, f) &= \int_{-\infty}^{\infty} x(t)w(t-\tau)\mathrm{e}^{-\mathrm{j}2\pi ft}\,\mathrm{d}f \\ &= \int_{-\infty}^{\infty} x(t)w^*_{t,f}(t)\,\mathrm{d}t\end{aligned} \tag{9}$$

where $w^*_{t,f}(t) = w(t-\tau)\mathrm{e}^{-2\pi ft}$. STFT analyses the signal $x(t)$ through a short-time window $w(t) : x(t)w(t-\tau)$, and then a Fourier transform is performed on this product using a complex exponential basis functions. The square modulus of STFT is referred to as the spectrogram

$$\mathrm{SPEC}_x(\tau, f) = |\mathrm{STFT}_x(\tau, f)|^2 \tag{10}$$

In this report, both CWT and STFT are used for coherence analysis and the performance of the two is compared.

2.1.2. Estimation of time–frequency coherence

In order to study the relationship between two non-stationary processes, definitions of cross spectrum and coherence are required. Given two processes $x(t)$ and $y(t)$ with their time–frequency representations $\mathrm{X}(\tau, f)$ and $\mathrm{Y}(\tau, f)$ (these can be based on either STFT or wavelet transforms), the time–frequency cross spectrum between them is defined as

$$S_{xy}(\tau, f) = X(\tau, f)Y^*(\tau, f) \tag{11}$$

and the auto spectra are given by

$$S_x(\tau, f) = |X(\tau, f)|^2 \tag{12}$$

$$S_y(\tau, f) = |Y(\tau, f)|^2 \tag{13}$$

The time–frequency based coherence, the square of the cross spectrum normalised by the individual auto spectra, is defined by

$$R^2_{xy}(\tau, f) = \frac{|S_{xy}(\tau, f)|^2}{S_x(\tau, f)S_y(\tau, f)} \tag{14}$$

The above definitions are straightforward and they follow a similar approach to that in Fourier analysis. In Fourier analysis, the spectra and the coherence can be estimated by virtue of the periodogram method in which a number of segments are averaged. However, in the case of time–frequency coherence problems arise when using averaging because there are two dimensions (time and frequency). It is unclear along which direction the smoothing should be done (Torrence and Compo, 1998). As noted in Torrence and Compo (1998), the coherence will have an identical value of one at all times and frequencies without smoothing. Localised smoothing allows wavelet coherence to be estimated for a single trial (Gurley et al., 2003; Lachaux et al., 2002). Here a series of repeat trials is analysed by averaging across trials without smoothing within trials. The estimate of the coherence is defined in this case as

$$\hat{R}^2_{xy}(\tau, f) = \frac{|\hat{S}_{xy}(\tau, f)|^2}{\hat{S}_x(\tau, f)\hat{S}_y(\tau, f)} \tag{15}$$

where

$$\hat{S}_x(\tau, f) = \frac{1}{K}\sum_{k=1}^{K}|X_k(\tau, f)|^2 \tag{16}$$

$$\hat{S}_y(\tau, f) = \frac{1}{K}\sum_{k=1}^{K}|Y_k(\tau, f)|^2 \tag{17}$$

$$\hat{S}_{xy}(\tau, f) = \frac{1}{K}\sum_{k=1}^{K}X_k(\tau, f)Y_k^*(\tau, f) \tag{18}$$

Eqs. (15)–(18) outline the procedure for estimating time–frequency coherence. The two channels of data contain a series of repeated trials $\{x_1(t)\ldots x_k(t)\}$ and $\{y_1(t)\ldots y_K(t)\}$ that are recorded simultaneously. In each trial $x_k(t)$ and $y_k(t)$, the time–frequency representations $X_k(\tau, f)$ and $Y_k(\tau, f)$ are calculated and their squared magnitude $|X_k(\tau, f)|^2$ and $|Y_k(\tau, f)|^2$ (spectrogram or scalo-gram) as well as the cross spectrum $X_k(\tau, f)Y_k^*(\tau, f)$ are calculated. After averaging across these multiple trials, the estimates for auto spectra and cross spectrum are obtained and they lead to the estimate of the time–frequency based coherence as expressed in (15). The cross spectra consist of complex values, and the amplitude and phase spectra can be defined as the absolute value and angle, respectively.

2.1.3. Confidence intervals

In order to construct confidence intervals for the above time–frequency coherence some assumptions are required of the data. In Fourier analysis, the two time series are assumed to be stationary and a theoretical distribution (e.g. Gaussian) is used to approximate the probability density of the data.

However, because the time–frequency analysis contains temporal changes or time-varying information, the description of the statistics is confined to a localised interval (Priestley, 1996). The wavelet spectra have been compared to Fourier spectra in Perrier et al. (1995) and the variance of the wavelet spectra was analysed in Percival (1995). The wavelet spectrum based on continuous wavelet transform was studied in Li and Oh (2002); where it was concluded that the wavelet spectrum can represent the second-order statistical properties of random processes for stationary and some non-stationary processes. It was shown that the local wavelet spectrum follows the mean Fourier spectrum (Torrence and Compo, 1998). Based on this assumption, the wavelet power spectrum should be χ^2 distributed and confidence levels for the cross-wavelet spectrum can be derived from the square root of the product of two χ^2 distributions.

For the setting of confidence intervals for the time–frequency based coherence the notion of generalised coherence is used here Gish and Cochran (1988). Let $\mathbf{X} = \{X_k(\tau, f)\}_{k=1}^K$ and $\mathbf{Y} = \{Y_k(\tau, f)\}_{k=1}^K$ denote the complex time–frequency representation of a sequence of repeated trials. Then the estimate of the coherence in (15) can be denoted by

$$\hat{R}_{xy}^2(\tau, f) = \frac{|\langle \mathbf{X}, \mathbf{Y}\rangle|^2}{||\mathbf{X}||^2 \times ||\mathbf{Y}||^2} = \frac{|\sum_{k=1}^K X_k(\tau, f)Y_k^*(\tau, f)|^2}{\sum_{k=1}^K|X_k(\tau, f)|^2 \times \sum_{k=1}^K|Y_k(\tau, f)|^2} \tag{19}$$

where $\langle \mathbf{X}, \mathbf{Y}\rangle$ is the inner product of X and Y, defined by

$$\langle \mathbf{X}, \mathbf{Y}\rangle = \sum_{k=1}^K X_k(\tau, f)Y_k^*(\tau, f) \tag{20}$$

$||\mathbf{X}||^2 = \langle \mathbf{X}, \mathbf{X}\rangle$ and $||\mathbf{Y}||^2 = \langle \mathbf{Y}, \mathbf{Y}\rangle$ are the squared magnitudes of $\mathbf{X}$ and $\mathbf{Y}$. The time–frequency based coherence takes the values between 0 and 1 and in particular, $\hat{R}_{xy}(\tau, f) = 0$ if $\mathbf{X}$ and $\mathbf{Y}$ are orthogonal. If $\mathbf{X} = a\mathbf{Y}$ for any non-zero complex number a then $\hat{R}_{xy}(\tau, f) = 1$.

If the two processes are independent the coherence is particularly useful because no common signal component is present. Under the hypothesis that the two processes are independent Gaussian noise, thresholds corresponding to a particular probability can be set. The distribution of the coherence estimate (Gish and Cochran, 1988) is given by

$$Pr(R^2 \le r) = 1 - (1 - r)^{K-1}, \quad 0 \le r \le 1 \tag{21}$$

where $Pr(\cdot)$ denotes the probability, and r is the detection threshold. For a 95% confidence interval, $1 - (1 - r)^{K-1} = 0.95$, and the detection threshold is $r_{95\%} = 1–0.05^{1/(K-1)}$ An estimate which is less than this value is regarded as not significant.

The above construction of the confidence interval is based on the assumption that the two processes have independent Gaussian distribution. However, as pointed out in Gish and Cochran (1987), the distribution of the coherence estimate does not depend on the statistics of one of the two processes provided that the other process is Gaussian and the two processes are independent. This property shows that the coherence estimate is invariant with respect to the second channel statistics as long as one of the two independent processes is Gaussian. This assumption can be further weakened by a geometric argument that the process has spherically symmetric distribution (see Appendix A) instead of the stronger Gaussian assumption (Gish and Cochran, 1987; Sinno and Cochran, 1992).

2.2. Discrimination in frequency domain

This section considers the issue of frequency discrimination by CWT and STFT based coherence estimates. Theoretically the time–frequency resolution of the STFT and CWT is bounded by the Heisenberg box, centred at a given position with time and frequency widths defined as the root mean square spread of the transform basis functions in the time and frequency domain. This rectangular box illustrates the trade-off relationship between time and frequency (Akansu and Haddad, 2000; Cohen, 1995). Here, we consider the ability to resolve two nearby frequency components in noisy data using the above time–frequency estimates. Assume that two local maxima of coherence exist at frequencies f_1 and $f_2, f_2 \neq f_1$, we want to statistically test whether $f_1 \neq f_2$ or not.

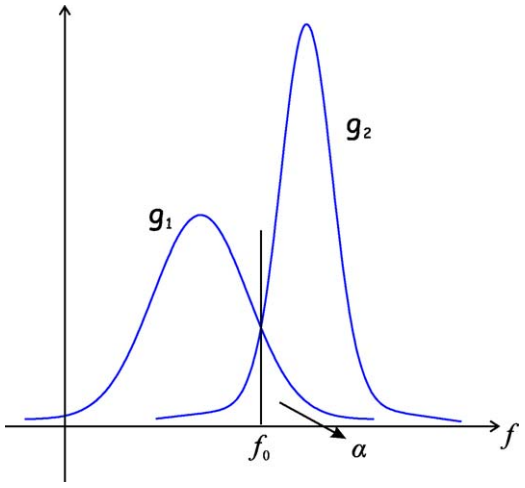

Fig. 2. Illustration of frequency discrimination test (see text for details).

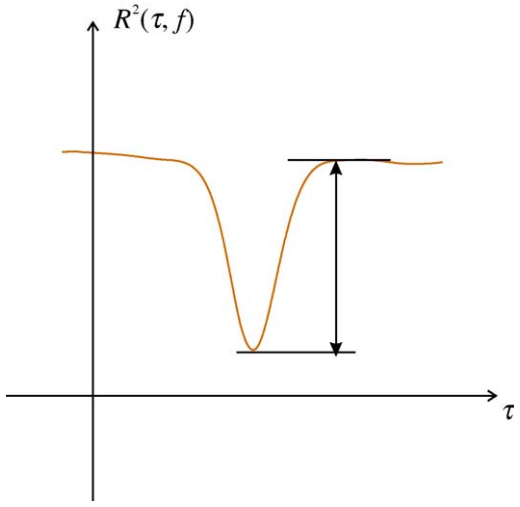

Fig. 3. Illustration of time discrimination test (see text for details).

A frequency discrimination test is important since it tells us the ability of the coherence estimator to discriminate two correlated components that are close in frequency. Using simulated data with localised coherent components at f_1 and f_2, $R^2(f_1)$ and $R^2(f_2)$, repeat runs can be used to obtain the distribution of the peak frequencies: $g_1(f)$ and $g_2(f)$ (see Fig. 2). To see if f_2 can be discriminated from f_1, we can choose an observation value $F = f_0$ where $g_1(f_0) = g_2(f_0)$ and use the following error probability as the discrimination criterion

$$Pr(F \geq f_0 | g_1) = \alpha \tag{22}$$

If a 5% error probability is selected, i.e. when $\alpha < 0.05$ we can say that the nearby frequency f_2 can be discriminated from f_1.

2.3. Discrimination in time domain

In this section, we consider the issue of time discrimination by CWT and STFT based coherence estimates. Coherence in the time dimension is usually reflected as correlation during a specific time interval. Fixing one interval and testing alongside a nearby interval (as used above for the frequency discrimination test) requires the width of each interval to be chosen in advance. An alternative approach, which is used here, is to have two processes correlated across the entire time range, with a small period covering the same time interval in each process having no correlation at all. This should result in a gap in the time–frequency coherence estimate. The width of this gap period is used to assess the time discrimination of the coherence estimate.

The coherence estimate at the chosen frequency will have a significant dip around the chosen gap but remain high in amplitude on either side of the gap (see Fig. 3). The distance between the minimum coherence value at the dip and the neighbouring (average) is used to quantify the time discrimination abilities of CWT and STFT coherence estimates. Simulated data with a fixed gap in each trial is used for this test. As the duration of the time gap in each trial is reduced a point will be reached where there is no significant difference in the two distributions describing the estimated coherence values in the gap and the average on either side. A t-test is used below to determine if the two distributions of coherence values have significantly different means for different values of time gap.

3. Results

3.1. Simulated data

In order to test the performance of the time–frequency coherence defined above, artificial data was generated to simulate the processes containing repeat trials. The two test time series are Gaussian white noise with sine waves embedded in each trial of the two processes. Three values of signal-to-noise ratio (SNR) are used, −10 dB, −15 dB and −20 dB. The Gaussian white noise used has unit variance and the amplitudes of sine wave in each trial are adjusted according to the value of SNR. The number of repeat trials is fixed for each value of SNR, at 20, 50 and 200, respectively. In general higher SNR will require a greater number of trials to reliably detect the signal (sine wave) in the presence of noise.

Fig. 4 shows a three-dimensional plot of the CWT based time–frequency coherence defined above, with SNR was chosen as −10 dB and 20 trials were used. The coherent signal consisted of 25 Hz sine waves embedded into each trial from 500 ms to 600 ms. The plane in the figure shows the 95% confidence interval calculated based on (21). A significant peak can be seen in the estimate between 500 ms and 600 ms and around 25 Hz in the time–frequency plane, as expected. This figure illustrates the localised nature (in both time and frequency) of the common sinusoidal component across the repeat trials in the two signals. Similar results are obtained from an STFT coherence estimate (not shown).

In Fig. 5, time–frequency coherence estimates are shown using STFT and CWT based coherence estimates, for two SNR settings, −15 dB with 50 trials, and −20 dB with 200 trials. Three different common sinusoidal components are embedded at different fixed times within each trial (see legend for details). Visual inspection of the results shows that both methods can detect the correlations. There are some qualitative differences

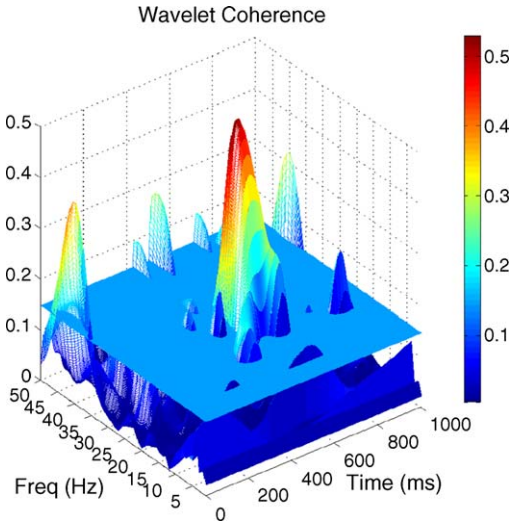

Fig. 4. Time–frequency coherence using CWT of two Gaussian white noise signals with a trial length of 1000 ms, and with a common sine wave of 25 Hz embedded from 500 ms to 600 ms in both channels in each trial. The SNR was −10 dB and 20 trials were generated with sampling rate 1 kHz. Morlet wavelet was used with $f_0 = 0.849$.

between the two estimators. The STFT estimates have a fixed Heisenberg box across the time–frequency plane. The CWT based estimates have a variable Heisenberg box, with narrower frequency resolution at low frequencies and narrower time resolution at higher frequencies. This shapes the significant areas in each estimates. The STFT has a larger magnitude at 5 Hz, whereas the CWT estimate has a larger magnitude at 25 Hz and 40 Hz. This suggests the estimates have different resolving abilities at different frequency ranges. This was verified using repeat runs with the same configuration, the STFT estimate consistently gave larger coherence values for the 5 Hz component.

To further characterise the resolving abilities of the two estimators, they were applied to simulated data where the frequency of the common component was varied systematically from 1 Hz to 50 Hz, Fig. 6. The data consists of 500 samples (0.5 s) with common sine waves embedded from 200 ms to 300 ms. For the STFT, we use two different window lengths of 100 ms and 150 ms, which gives a fundamental frequency resolution of 10 Hz and 6.7 Hz, respectively. The STFT estimate with 100 ms window length gives consistently higher coherence values when compared with the CWT estimate. The 150 ms window STFT estimate gives higher coherence values than the CWT at frequencies below 23 Hz, above this the CWT estimate gives higher values. Both approaches are sensitive to the wide range of sine wave frequencies embedded in the data. The four plots on the right of Fig. 6 show the time (upper) and frequency (lower) at which the maximal coherence occurred. Both approaches (STFT, 150 ms data window and CWT) detect a maximum between 200 ms and 300 ms, as expected. Frequency localisation in both methods is poor at the lowest frequencies. For the STFT estimate, a window length of 150 ms defines a frequency resolution of 6.7 Hz, this will explain the poor frequency localisation below 10 Hz in the STFT estimate. The CWT estimate at lower frequencies may suffer from edge effects, as the broader wavelets extend to areas outside the data window. This phenomenon is referred to as the cone of influence (COI) (Torrence and Compo, 1998). In addition, the test sine wave is only 100 ms duration, which does not cover a complete oscillatory cycle at frequencies below 10 Hz. Frequency localisation may improve if longer periods of coherent activity are to be detected, this could be verified with additional simulations similar to those used here.

3.2. Frequency discrimination test

The method described above for frequency discrimination was applied to simulated data (SNR −10 dB, 20 trials). The reference frequency was fixed at $f_1 = 20$ Hz and the distribution of the frequency of maximal coherence for 100 independent sets approximated by a normal distribution (see Fig. 7). The second frequency, f_2, was systematically varied and 100

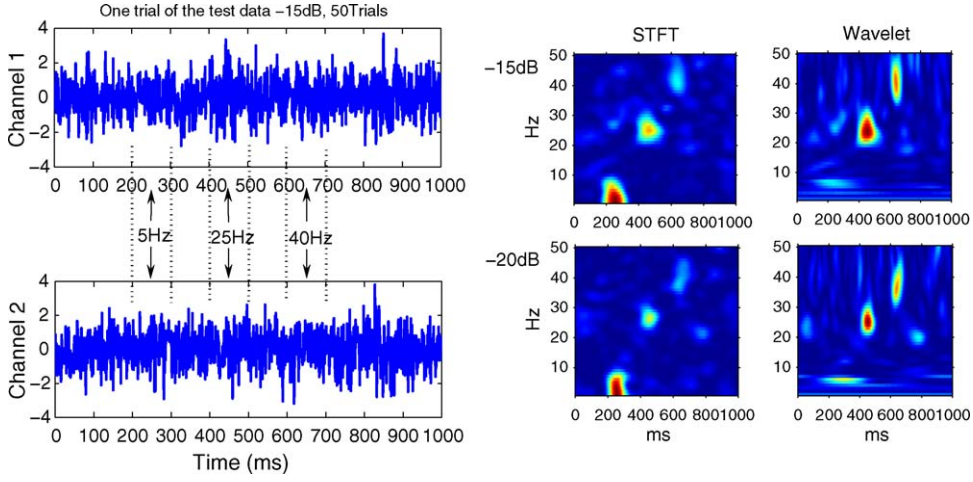

Fig. 5. Time–frequency coherence using STFT and CWT with SNR ratios of −15 dB and −20 dB. Three sine wave components were embedded into both Gaussian white noise signals in each trial at 200–300 ms with 5 Hz, 400–500 ms with 25 Hz and 600–700 ms with 40 Hz. Different trials were generated for different SNRs with sampling rate 1 kHz, 50 trials at −15 dB and 200 trials at −20 dB. In the figure, the left column used STFT and the right column used the CWT, with (top) SNR of 15 dB and (bottom) −20 dB. In the STFT, a Gaussian data window of width 300 ms with maximum overlap points between each time step was used. The CWT used a Morlet wavelet with $f_0 = 0.849$.

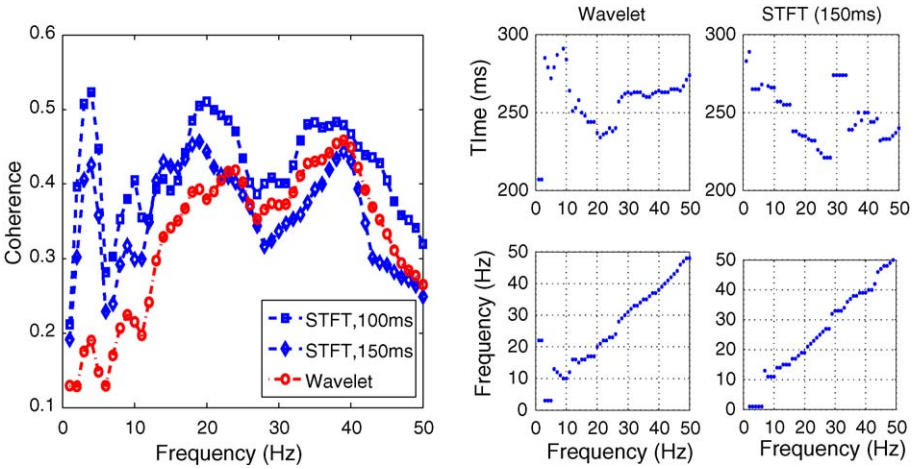

Fig. 6. Time–frequency coherence estimates for simulated data with varying frequency of common sine wave. Data was generated using two white noise series of length 500 ms with one single period of a sine wave embedded from 200 ms to 300 ms, with frequencies varying from 1 Hz to 50 Hz. Coherence is calculated at each frequency using STFT and CWT estimates. The SNR is −15 dB and 50 trials are included. Left, comparison of peak coherence between CWT and STFT (with window lengths of 100 ms and 150 ms) based estimates. Right, time and frequency localization of estimates. The left column is for CWT and the right is for STFT (150 ms data window). The top two plots are time where the coherence reaches its maximum, the bottom two plots are the frequencies where the coherence reaches a maximum.

independent coherence estimates generated at each value, which were approximated by a normal distribution. A 5% error probability was selected as the discrimination criterion, i.e. when the distributions overlap by less than 5% we conclude that the nearby coherence peak at frequency f_2 represents a different component from f_1. Fig. 7 shows that for a reference frequency $f_1 = 20$ Hz the critical frequency is around $f_2 = 28$ Hz, for the STFT, and $f_2 = 25$ Hz for the CWT. Therefore, for this simulated data, the CWT exhibits better frequency discrimination than the STFT based coherence estimate.

3.3. Time discrimination test

Using the time discrimination test described above, 100 independent samples were generated for time gaps of 5–80 ms, (Fig. 8). The top left plot shows the CWT coherence with different gap widths from 10 to 80 ms in 10 ms steps using the CWT estimate. There is a systematic increase in the drop in coherence as the time gap increases. The lower time–frequency plots show the average coherence estimates for time gaps of 5 ms, 10 ms, 20 ms and 50 ms at a coherent frequency of 20 Hz. The CWT has a narrower strip in the frequency domain than the STFT estimate. Visual inspections suggest that the STFT estimate is more sensitive to gaps in the data. However, application of the *t*-test described above (upper right plot), give consistently higher *t*-values for the CWT method, suggesting the CWT may be more sensitive to gaps in the data. Both coherence estimates are sensitive to gaps in the data of greater than 5 ms.

3.4. Data with unmatched sine waves

All the above simulated data used sine waves symmetrically embedded into each trial of both channels. To test the effects of inhomogeneity between trials, this section uses simulated data with unmatched sine waves. In one channel 25% of trials have the sine wave components deleted at random, the other channel remains unaffected. Results are in Fig. 9, using 20 Hz sine waves, −10 dB SNR, 20 trials. Both STFT and CWT estimates identify

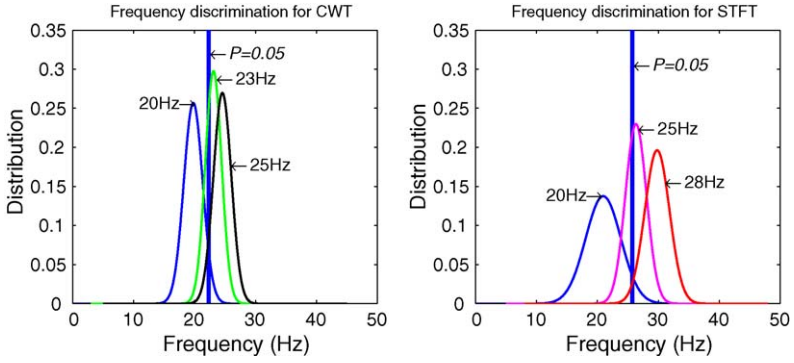

Fig. 7. Histograms showing the distribution of peak coherence frequency for 100 independent sets of test data (SNR −10 dB, 20 trials). A fixed reference frquency of $f_1 = 20$ Hz was used, and the distribution of nearby frequencies *i* plotted for comparison. A 5% error probability was selected as the discrimination criterion, indicated by the vertical line. For the STFT the 5% criterion is satisfied for frequencies about 28 Hz, for the CWT is satisfied for frequencies about 26 Hz.

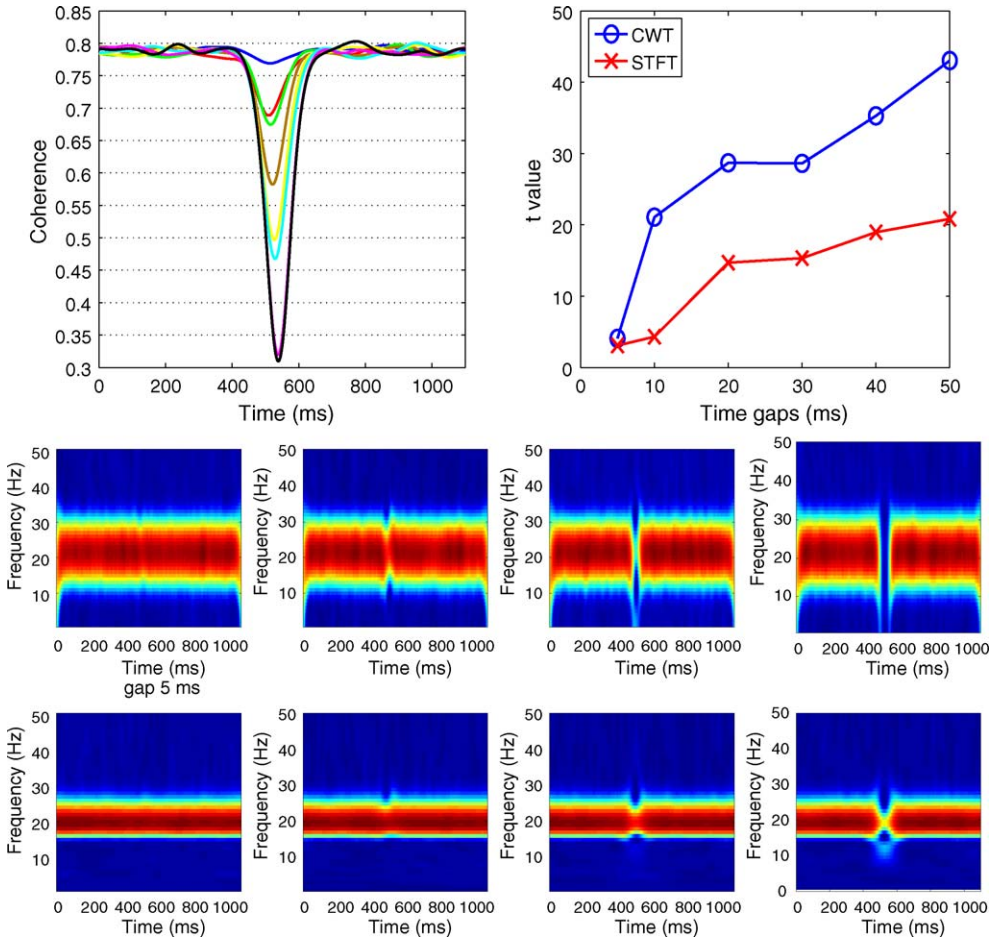

Fig. 8. Time discrimination test for data with time gaps of 5 ms, 10 ms, 20 ms, 30 ms, 40 ms, 50 ms, 60 ms, 70 ms and 80 ms starting from 500 ms at a fixed frequency of 20 Hz. Top left, coherence averaged across 100 independent samples using CWT, the eight lines from top to bottom correspond to time gaps from 10 ms to 80 ms. Top right, calculated *t*-value as described in the text. Middle panel, averaged coherence for STFT. Bottom panel, averaged coherence for CWT, from the left to the right, the estimates corresponds to time gaps of 5 ms, 10 ms, 20 ms and 50 ms. The SNR is −15 dB and the trial number is 50. The choice of the analysing window for STFT and wavelet for CWT is the same as in Fig. 5.

the 20 Hz correlation between 200 ms and 300 ms. However, additional peaks are present, suggesting that inhomogeneity can create coherence values, which are not present in the signals. In this single run, these subsidiary peaks appear more prominent in the CWT based estimate.

3.5. Application to neural and muscular signals

3.5.1. Movement-related signals

This section considers application of the time–frequency coherence analysis to movement related signals in the form of

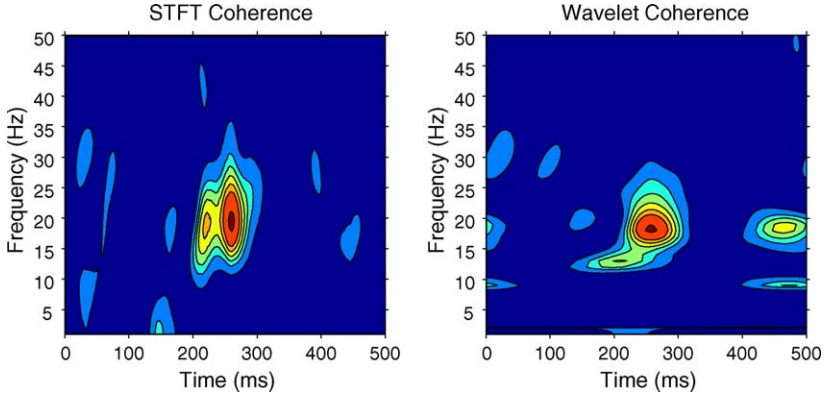

Fig. 9. Coherence analysis for simulated data with unmatched sine waves. The data consists of 20 trials, 200 ms duration, SNR −10 dB with 20 Hz sine waves embedded between 200 ms and 300 ms, 25% of the sine wave components are randomly deleted in one channel. The choice of the analysing window for STFT and wavelet for CWT is the same as in Fig. 5. Regions above the 95% confidence interval are shown. Left: STFT method; right: CWT method.

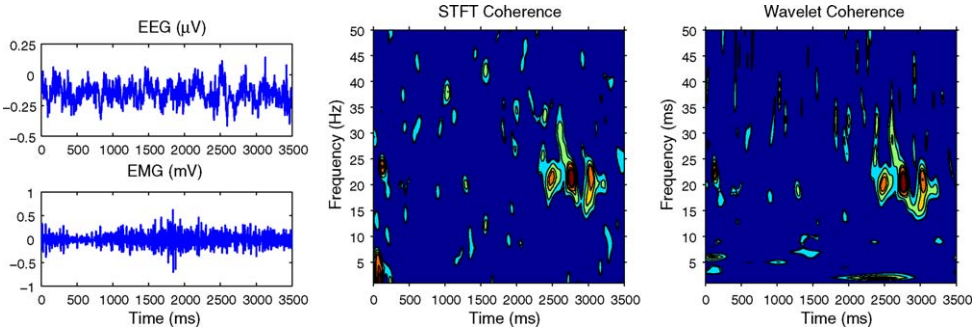

Fig. 10. Analysis using STFT and CWT coherence on EEG and EMG during a wrist flexion extension task. The choice of the analysing window for STFT and wavelet for CWT is the same as in Fig. 5. Only regions above the 95% confidence interval are shown.

simultaneous recordings of scalp EEG and muscle EMG during an externally cued wrist extension/flexion task. The data is taken from the study of Halliday et al. (1998), where a detailed description of the experimental protocol can be found. Briefly, EEG was recorded from the contralateral sensorimotor cortex and EMG from the wrist extensor muscles while the subject made repeated wrist extension flexion movements in response to external auditory cues. The movement phase lasted around 1.5 s, this was followed by a hold phase of 2–3 s duration. Fig. 10 left shows EEG and EMG signals from a single trial, wrist extension occurs from 0 s to 1.5 s, maintained wrist flexion from 1.5 s to 3.5 s. The data set analysed here consists of 40 repeat trials from a single subject, before analysis both channels have their mean subtracted and a linear trend removed, and the EMG is full wave rectified.

STFT and CWT coherence estimates between EEG and EMG are shown in Fig. 10. The dominant features in the CWT coherence are a peak of magnitude 0.20 at 2.8 s, 20 Hz, other components are at 2.5 s, 20 Hz and 3.0 s, 21 Hz. In the STFT coherence the dominant feature is 2.8 s, 22 Hz, other peaks are at 2.3 s, 20 Hz and 3.2 s, 20 Hz. Both approaches indicate a clear correlation between contralateral EEG and extensor EMG during maintained wrist extension from 2.5 s to 3.0 s. The estimated phase spectrum (not shown) at a frequency of 20 Hz indicates that the two signals are out of phase during this time period. Apart from these dominant features in the time–frequency plane, other more localised peaks are present. Both STFT and CWT have coherence peaks at movement onset around 0.1 s at 5 Hz and 23 Hz. The effects of time scaling can be seen in the CWT based estimate, where isolated peaks at low frequency are well localised in frequency (and dispersed in time), whereas isolated peak at high frequency are well localised in time (and dispersed in frequency).

The SNR, calculated as the ratio of the power from 1 Hz to 250 Hz and from 251 Hz to 500 Hz, is <-10.2091 dB, this compared broadly with the SNR used previously with simulated data. The major concentration of coherence has three peaks at frequencies between 20 Hz and 22 Hz, and times 2.3–2.5 s, 2.8 s. Comparison with the previous time and frequency discrimination tests suggests that these peaks cannot be said to have a different frequency, but may represent different time periods of coherent activity.

3.5.2. *Tremor-related signals*

Deep brain stimulation is regarded as an effective clinical treatment for Parkinson's disease, it also provides an opportunity to study neuronal activity recorded from electrodes implanted for stimulation of the subthalamic nucleus (STN) (Liu et al., 2002, 2003). The second sample application is to simultaneous recordings of STN local field potentials (LFPs) and surface EMGs from the forearm extensor muscle during Parkinsonian rest tremor.

The 66 s of STN and EMG data was partitioned into 33 segments, each 2 s. Fig. 11 (left) shows a period of typical LFP and EMG activity in a single trial. The STFT and CWT coherence estimates both indicate a broad band of coherence across the 2 s

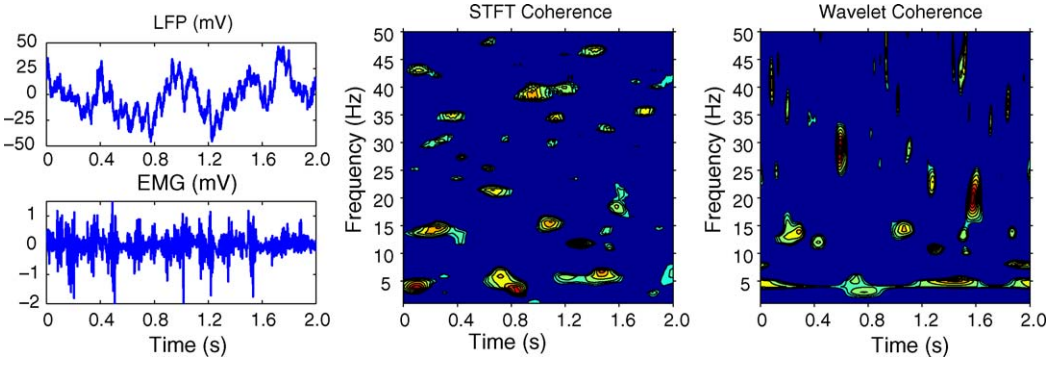

Fig. 11. STFT and CWT coherence between STN LFP and EMG signals during Parkinsonian rest tremor. Only regions above the 95% confidence interval are shown. The choice of the analysing window for STFT and wavelet for CWT is the same as in Fig. 5.

time scale at the tremor frequency of 3–7 Hz, in accordance with previous findings from spectral analysis of Parkinsonian data (Liu et al., 2002; Wang et al., 2001). There is an indication that the 3–7 Hz coherence exhibits some temporal structure, e.g. in the STFT coherence estimate the coherence peaks at times 0.12 s, 0.85 s and 1.47 s. In the CWT based estimate the peak times in this frequency band are 0.01 s, 0.79 s and 1.47 s, thus both estimates identify three main concentrations of coherence at the tremor frequency. This further suggests that the coherent oscillations between STN and EMG vary over time. However, the precise details of this are difficult to characterise from the present analysis, which split a single long record into 2 s blocks. Other distinct coherence peaks are present in the coherence estimates, particularly in the 10–15 Hz frequency band and the 20–30 Hz frequency band. Comparison with the analysis of EEG-EMG in the previous section from a healthy subject indicates different patterns of oscillatory activation exist between healthy subjects and Parkinson's disease.

4. Discussion

A framework has been presented for time–frequency coherence analysis using both Fourier (STFT) and Wavelet (CWT; Morlet) transforms, which relies on averaging across repeat trials. The techniques have been used to examine time dependency in experimental data consisting of EEG-EMG during voluntary wrist extension/flexion, and LFP-EMG during Parkinsonian tremor. For these data sets, both methods were able to successfully detect coherent components in the time–frequency plane. The first experimental data set (EEG-EMG) demonstrated the presence of 15–30 Hz, β, oscillations during maintained position holding, in agreement with previous studies (Halliday et al., 1998; Kilner et al., 2000). Analysis of the second experimental data set examined the relationship between LFP and EMG during Parkinsonain tremor. This showed a continuous band of coherence at the tremor frequency (3–7 Hz), as well as other isolated coherence peaks in the 10–15 Hz and 20–30 Hz range. These two examples illustrate the usefulness of a time–frequency coherence in studying how correlation evolves with time, within a repeat trial experimental protocol.

A method to estimate confidence intervals for time–frequency coherence estimates is given, based on the concept of generalised coherence. Averaging across repeat trials is an integral part of the present framework. The value of confidence limit is determined by the number of trials, which are averaged. A low number of trials will result in a large confidence limit. It is not possible to estimate coherence from spectrograms of scalograms, which have not been smoothed (Torrence and Compo, 1998). The assumption underlying the present framework is that the pattern of correlation follows a similar time evolution across repeat trials. Results from simulated data suggest that non homogeneity between trials may result in additional spurious peaks, which will complicate interpretation.

Tests were developed to assess the time and frequency discrimination capabilities of the present methods. Using results from 100 independent sets of simulated data, we have shown that the CWT method has a better frequency resolution than STFT, for our chosen frequency of 20 Hz, using a 5% error probability for the discrimination of two nearby frequencies. For time discrimination, both methods can resolve time gaps above 5 ms, which may be a useful property in time–frequency analysis. A *t*-test analysis (based on the magnitude of the dip in coherence at a gap in the common sine wave component) suggested the CWT method may have an improved performance over the STFT. The actual resolution in the time–frequency plane will be determined by the Heisenberg uncertainty principle, this can be usefully illustrated using Heisenberg boxes (Addison, 2002). The statistical approaches used here could be broadened to test other issues related to discrimination in the time–frequency plane.

The STFT has been extensively applied to analyse non-stationary biomedical signals (Lin and Chen, 1996). The STFT uses a fixed time window across the entire time–frequency plane, recently wavelet methods have become more popular for time–frequency analysis, (e.g. Addison, 2002; Qian, 2002; Lachaux et al., 2002). However as pointed out in Bruns (2004) Morlet wavelet and Fourier methods are formally equivalent. Our results support this conclusion, and demonstrate that STFT and CWT based coherence estimates provide a very similar description of the same data. Indeed, in the present study the STFT based coherence estimates generally have larger magnitudes than the CWT based estimates at lower frequencies, although a number of factors may contribute to this (e.g. sensitivity, bias, parameter values). Our results suggest both methods should be evaluated when undertaking a time–frequency coherence analysis.

Although the current study is confined to bivariate EEG, LFP and EMG data, this approach could be applied to data from in vivo multi-unit recordings, including multi unit spike train data.

Acknowledgment

J.F. was partially supported by grants from UK EPSRC (GR/R54569), (GR/S20574), and (GR/S30443). D.H. was partially supported by grants from UK EPSRC (GR/R12350). X.L. was partially supported by grants from UK MRC (GI 71766).

Appendix A. Spherically symmetric processes

Given a complex random processes denoted by $\{\mathbf{a} = x_n + \mathrm{i}y_n\}_{i=1}^{N}$, if the probability density function of **a** can be expressed as

$$f\mathbf{a}(x_1, \ldots, x_N, y_1, \ldots, y_N) = f_{\mathrm{ss}}\left(\sum_{n=1}^{N}(x_n^2 + y_n^2)\right) \tag{23}$$

where f_{ss} is a one-dimensional function, i.e. the value of the density function depends only on the distance from the origin and not on the direction, then a is said to be spherically symmetric. For detailed discussion about the property spherically symmetric, one can refer to Gish and Cochran (1987).

References

Addison PS. The illustrated wavelet transform hand book. IOP Publishing Ltd; 2002.

Akansu A, Haddad R, editors. Multiresolution signal decomposition: transforms, subbands and wavelets. Boca Raton: Academic Press; 2000.

Andrew C, Pfurtscheller G. Event-related coherence as a tool for studying dynamic interaction of brain regions. Electroencephalogr Clin Neurophysiol 1996;98(2):144–8.

Bruns A. Fourier–Hilbert- and wavelet-based signal analysis: are they really different approaches? J Neurosci Methods 2004;137(11):321–32.

Cohen L, editor. Time–frequency analysis. PTR Prentice Hall; 1995.

Feng J, editor. Computational neuroscience: a comprehensive approach. Boca Raton: Chapman and Hall/CRC Press; 2004.

Gish H, Cochran D. Invariance of the magnitude-squared coherence estimate with respect to second-channel statistics. IEEE Trans Acoust Speech Signal Process ASSP-35 1987;12:1774–6.

Gish H, Cochran D. Generalized coherence. In: International conference on acoustics, Speech, and Signal Processing, vol. 5, April; 1988. p. 2745–8.

Grosse P, Cassidy MJ, Brown P. EEG-EMG, MEG-EMG and EMG-EMG frequency analysis: physiological principles and clinical applications. Clin Neurophysiol 2002;113(10):1523–31.

Gurley K, Kijewski T, Kareem A. First-and higher-order correlation detection using wavelet transforms. J Eng Mech 2003;129(2):188–201.

Halliday DM, Conway BA, et al. Using electroencephalography to study functional coupling between cortical activity and electromyograms during voluntary contractions in humans. Neurosci Lett 1998;241:5–8.

Horton PM, Bonny L, Nicol A, Kendrick K, Feng J. Applictions of multivariate analysis of variances (manova) to multi-electrode array data. J Neurosci Methods 2005;146(13):22–41.

Karlsson JS, Ostlund N, et al. An estimation of the influence of force decrease on the mean power spectral frequency shift of the emg during repetitive maximum dynamic knee extensions. J Electromyogr Kinesiol 2003;13(5):461–8.

Kilner J, Baker S, Salenius S, Hari R, Lemon R. Human cortical muscle coherence is directly related to specific motor parameters. J Neurosci 2000;20(13):8838–45.

Kronland-Martinet R, Morlet J, Grossmann A. Analysis of sound patterns through wavelet transforms. Int J Pattern Recognit Artif Intell 1987;1(2):97–126.

Lachaux J-P, Lutz A, et al. Estimating the time-course of coherence between single-trial brain signals: an introduction to wavelet coherence. J Neurophysiol Clin 2002;32:157–74.

Lambertz M, Vandenhouten R, et al. Phase transitions in the common brainstem and related systems investigated by nonstationary time series analysis. J Auton Nerv Syst 2000;78(2–3):141–57.

Lee D. Analysis of phase-locked oscillations in multi-channel single-unit spike activity with wavelet cross-spectrum. J Neuro Methods 2002;115(1):67–75.

Li T, Oh H. Wavelet spectrum and its charaterization property for random processes. IEEE Trans Inform Theory 2002;48(11):2922–37.

Lin Z, Chen J. Advances in time–frequency analysis of biomedical signals. Crit Rev Biomed Eng 1996;24(1):1–72.

Liu X, Ford-Dunn HL, Hayward G, Nandi D, Miall R, Aziz T, et al. The oscillatory activity in the parkinsonian subthalamic nucleus investigated using the macro-electrodes for deep brain stimulation. Clin Neurophysiol 2002;113(13):1667–72.

Liu X, Rowe J, Nandi D, Hayward G, Parkin S, Stein J, et al. Localisation of the subthalamic nucleus using radionics image fusion and stereoplan combined with field potential recording. Clin Neurophysiol 2003;76(13):63–73.

Mima T, Hallett M. Electroencephalographic analysis of cortico-muscular coherence: reference effect, volume conduction and generator mechanism. Clin Neurophysiol 1999;110(11):1892–9.

Mima T, Steger J, et al. Electroencephalographic measurement of motor cortex control of muscle activity in humans. Clin Neurophysiol 2000;111(2):326–37.

Percival DB. On estimation of the wavelet variance. Biometrika 1995;82(3):619–31.

Perrier V, Philipovitch T, Basdevant C. Wavelet spectra compared to fourier spectra. J Math Phys 1995;36(3):1506–19.

Pezaris JS, Sahani M, Andersen RA. Spike train coherence in macaque parietal cortex during a memory saccade task. Neurocomputing 2000;32–33(June):953–60.

Pope MH, Aleksiev A, et al. Evaluation of low back muscle surface EMG signals using wavelets. Clin Biomech 2000;15(8):567–73.

Priestley MB. Wavelets and time-dependent spectral analysis. J Time Ser Anal 1996;17(1):86–103.

Qian S. Introduction to time–frequency and wavelet transforms. New Jersey: Prentice Hall PTR; 2002.

Samar VJ. Wavelet analysis of neuroelectric waveforms. Brain Lang 1999;66:1–6.

Senhadji L, Wendling F. Epileptic transient detection: wavelets and time–frequency approaches. Neurophysiol Clin 2002;32(3):175–92.

Shibata T, Shimoyama I, et al. The synchronization between brain areas under motor inhibition process in humans estimated by event-related EEG coherence. Neurosci Res 1998;31(4):265–71.

Sinno D, Cochran D. Invariance of the generalized coherence estimate with respect to reference channel statistics. In: IEEE international conference on acoustics, speech, and signal processing, vol. 2, March; 1992. p. 505–8.

Slobounov S, Tutwiler R, et al. Human oscillatory brain activity within gamma band 30–50 hz induced by visual recognition of non-stable postures. Cognitive. Brain Res 2000;9(2):177–92.

Tate A, Nicol A, Fischer H, Segonds-Pichon As, Feng J. Lateralised local and global encoding of face stimuli by neural networks in the temporal cortex. In: Annual meeting of neuroscience (oral presentation); 2005.

Torrence C, Compo GP. A pratical guide to wavelet analysis. Bull Am Meteo Soc 1998;79(1):61–78.

Torrence C, Webster PJ. Interdecadal changes in the ENSO-Monsoon system. J Climate 1999;12(8):2679–90.

Wang S, Liu X, Yianni J, Christopher Mi all R, Aziz T, Stein J. Optimising coherence estimation to assess the functional correlation of tremor-related activity between the subthalamic nucleus and the forearm muscles. J Neurosci Methods 2001;136(13):197–205.